

Optical Phonons in $\text{KCl}_{1-x}\text{Br}_x$ and $\text{K}_{1-x}\text{Rb}_x\text{I}$ Mixed Crystals

J. H. FERTEL AND C. H. PERRY*

Spectroscopy Laboratory† and Research Laboratory of Electronics,‡ Massachusetts Institute of Technology, Cambridge, Massachusetts 02139

The infrared lattice-vibrational spectra of mixed crystals of $\text{KCl}_{1-x}\text{Br}_x$ and $\text{K}_{1-x}\text{Rb}_x\text{I}$ have been observed at temperatures down to 80°K. The results were obtained from thin-film transmission measurements and Kramers-Kronig analyses of reflection data. A classical oscillator model was used to fit the reflectivity curves for the pure end members. The $\text{KCl}_{1-x}\text{Br}_x$ system shows the normal "one-mode" behavior. Two infrared-active phonons occur in the $\text{K}_{1-x}\text{Rb}_x\text{I}$ system, and this is the first observation of this type of behavior in an alkali halide mixed crystal. The applicability of several theoretical models is discussed, and the various criteria for one- and two-mode behavior are evaluated.

I. INTRODUCTION

TWO types of behavior are normally observed for the normal modes of mixed crystals. In one class of mixed crystal systems, a single lattice band appears whose frequency varies continuously from the frequency characteristic of one end member to that of the other end member. The mode strength remains approximately constant, while the damping increases to a maximum in the region of the 50-50 crystal. This is called "one-mode" behavior and has been reported for several alkali halide crystals,^{1,2} $\text{Ni}_{1-x}\text{CO}_x\text{O}$,³ $(\text{Ca},\text{Ba})_{1-x}\text{Sr}_x\text{F}_2$,^{4,5} and $\text{Cd}_x\text{Zn}_{1-x}\text{S}$.⁶

In a second class of mixed crystals, two bands appear at frequencies close to those of the end members, the relative strength of each mode being approximately equal to the fractional formula weight of each component. This is called "two-mode" behavior. Two-mode behavior has been reported only for covalent materials, such as $\text{GaAs}_{1-x}\text{P}_x$,^{7,8} $\text{InAs}_{1-x}\text{P}_x$,⁹ $\text{Ge}_{1-x}\text{Si}_x$,¹⁰ $\text{ZnS}_x\text{Se}_{1-x}$,¹¹ and $\text{CdS}_{1-x}\text{Se}_x$.¹² Until recently, alkali

halide mixed crystals have shown exclusively one-mode behavior.

Several criteria have been proposed to predict the appearance of one- or two-mode behavior in a given mixed crystal. Lucovsky, Brodsky, and Burstein¹³ (LBB) made a study of linear chain models and concluded that two-mode behavior would be observed in the crystal $AB_{1-x}C_x$ (with $m_C > m_B$) if the substitution of C for B in AB produces a gap mode and if the substitution of B for C in AC produces a localized mode. For a one-dimensional chain, these local and gap modes will occur if A is heavier than B , provided that the lighter end-member compound AB has a gap in its phonon spectrum between the optical and acoustic branches. In the case of a three-dimensional crystal, the situation is more complicated, however, as local and gap modes arise only when the ratio of substituting to substituted masses is between certain critical values.¹⁴

Chang and Mitra¹⁵ presented a model from which they derived the criterion that two-mode behavior will result if $m_B < \mu_{AC}$ [where $\mu_{AC} = m_A m_C / (m_A + m_C)$]. This restriction contains the local-gap mode conditions for a mixed linear chain, but not those for a three-dimensional mixed crystal. For example, if this inequality is satisfied, the local-mode frequency of AB in AC at $x=1$ will be higher than the TO frequency of AC , but it will not necessarily be higher than the LO frequency of AC . Therefore, a true local mode might not arise.

Attempts have also been made¹³ to relate the occurrence of one- or two-mode behavior to overlap of the end-member reflection bands which extend from the zone center TO to LO frequencies. Mixed crystal systems which exhibit frequency overlap always show one-mode behavior. The reverse is not true, however. One-mode behavior is also observed for some systems in which there is no frequency overlap, e.g., $\text{GaAs}_{1-x}\text{Sb}_x$ ¹⁶

Chang, in *Proceedings of the International Conference on II-VI Semiconducting Compounds, Providence, 1967*, edited by D. G. Thomas (W. A. Benjamin, Inc., New York, 1968), pp. 1150-1163.

¹³ G. Lucovsky, M. Brodsky, and E. Burnstein, in *Localized Excitations in Solids*, edited by R. F. Wallis (Plenum Press, Inc., New York, 1968), p. 592.

¹⁴ S. S. Jaswal, Phys. Rev. **137**, A302 (1965).

¹⁵ I. F. Chang and S. S. Mitra, Phys. Rev. **172**, 924 (1968).

¹⁶ R. F. Potter and D. L. Stierwalt, in *Proceedings of the Seventh International Conference on the Physics of Semiconductors, Paris, 1964* (Academic Press Inc., New York, 1965), p. 1111.

* Present address: Department of Physics, Northeastern University, Boston, Mass.

† This laboratory is supported in part by the National Science Foundation Grant No. GP-4923.

‡ This work is supported in part by the Joint Services Electronics Program [Contract No. DA28-043-AMC 02536(E)], and by the U. S. Air Force [ESD Contract No. AF19(628)-6066].

¹ F. Kruger, O. Reinkober, and E. Koch-Hohn, Ann. Physik **85**, 110 (1928).

² R. M. Fuller, C. M. Randall, and D. J. Montgomery, Bull. Am. Phys. Soc. **9**, 644 (1964).

³ P. J. Gielisse, J. N. Plendl, L. C. Mansur, R. Marshall, S. S. Mitra, R. Mykolajewycz, and A. Smakula, J. Appl. Phys. **36**, 2447 (1965).

⁴ R. K. Chang, B. Lacina, and O. S. Pershan, Phys. Rev. Letters **17**, 755 (1966).

⁵ H. W. Verleur and A. S. Barker, Jr., Bull. Am. Phys. Soc. **12**, 81 (1966).

⁶ G. Lucovsky, E. Lind, and E. A. Davis, in *Proceedings of the International Conference on II-VI Semiconducting Compounds, Providence, 1967*, edited by D. G. Thomas (W. A. Benjamin, Inc., New York, 1968), pp. 1150-1163.

⁷ H. W. Verleur and A. S. Barker, Jr., Phys. Rev. **149**, 715 (1966).

⁸ Y. S. Chen, W. Shockley, and G. L. Pearson, Phys. Rev. **151**, A648 (1966).

⁹ F. Oswald, Z. Naturforsch **14a**, 374 (1959).

¹⁰ D. W. Feldman, M. Ashkin, and J. H. Parker, Jr., Phys. Rev. Letters **17**, 1209 (1966).

¹¹ O. Brafman, I. F. Chang, G. Lengyel, S. S. Mitra, and E. Carnall, Jr., Phys. Rev. Letters **19**, 1120 (1967).

¹² J. F. Parrish, C. H. Perry, S. S. Mitra, O. Brafman, and I. F.

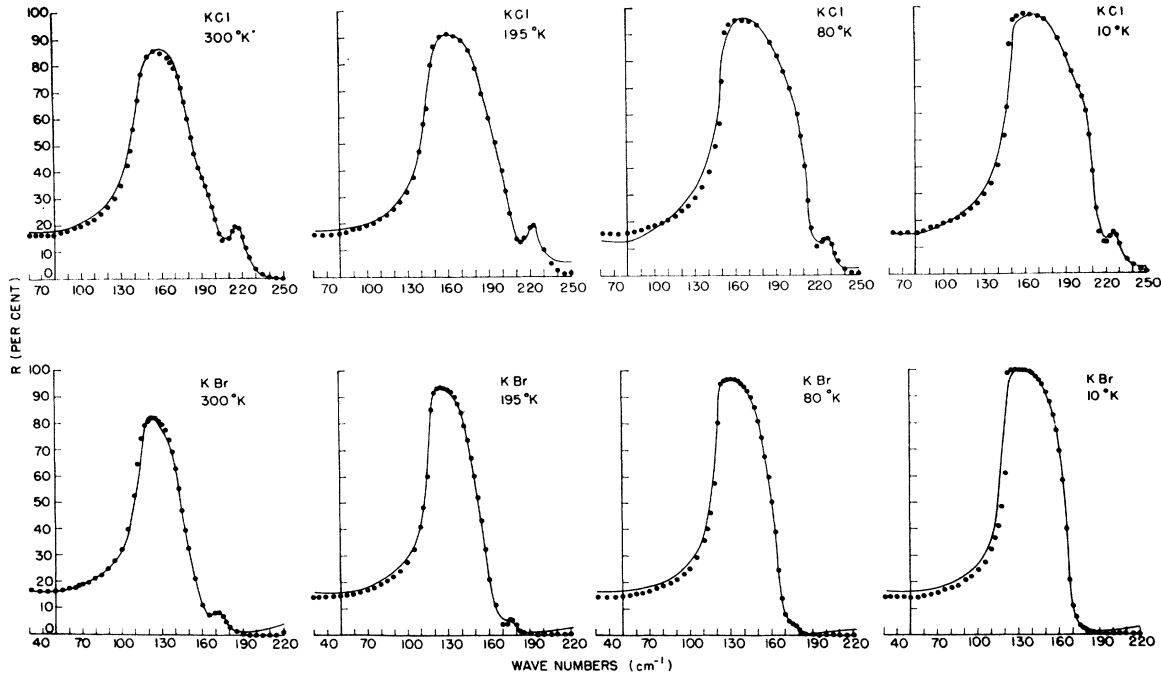


FIG. 1. Reflectivity spectra of KBr and KCl at several temperatures; solid line denotes those observed, dotted line those calculated from the classical oscillator model.

and $Se_{1-x}Te$.¹⁷ It appears, therefore, that this condition by itself is not sufficient to predict the number of modes.

Examination of the properties of the alkali halides shows that Chang and Mitra's criterion ($m_B < \mu_{AC}$) is satisfied by $K_{1-x}Rb_xI$, $K_{1-x}Rb_xBr$, and $RbCl_{1-x}Br$. Since KI and KBr are known to have gaps in their phonon spectra,¹⁸ $K_{1-x}Rb_xI$ and $K_{1-x}Rb_xBr$ also satisfy the criterion of LBB. It is not known, however, whether RbCl has a gap in its phonon spectrum,

although the large mass difference between Rb and Cl makes that probable. The only mixed system for which there is no frequency overlap between the end-member reflection bands is $K_{1-x}Rb_xI$, and this indeed turns out to be the only one for which two modes are observed.

II. EXPERIMENTAL PROCEDURE

The interferometer and detector used for this measurement have been described elsewhere.¹⁹ Reflection

TABLE I. Dispersion constants for alkali halides from classical oscillator fits.

	TO (Γ)																e^*/e
	S_T	ω_T	ω_{Tr}^a	γ_T	γ_{Tr}^a	S_1	ω_1	γ_1	S_2	ω_2	γ_2	ϵ_∞	ϵ_0	ω_L	ω_{LST}		
KCl (300°)	215	143	142	5	4.52	55	189.5	31	41	210.5	14.5	2.22	4.6	203	206	0.77	
KCl (195°)	223	147	146	3	3.36	48	190	32	48	216	18	2.22	4.63	210	213		
KCl (80°)	228	151	150	1.5	1.95	41	193	40	35	222.5	14	2.22	4.57	215	215		
KCl (10°)	238	150	151	1.0	1.36	37	193	30	36	221.5	14	2.22	4.59	214.5	214		
KBr (300°)	172	113	114	5	4.67	42	150	28	36.5	169	15	2.43	4.9	158	161	0.74	
KBr (195°)	170	117	118	1.5	2.83	39	150	33	28	172	10	2.43	4.64	160	161		
KBr (80°)	174	120	122	0.8	1.59	31	156	28	18	174	12	2.43	4.58	164	164		
KBr (10°)	174	122	123	0.1	0.86	24	157	28	19	176	23	2.43	4.5	165.5	166		
KI (300°)	147	103.5	102	6.6	6.22	50	136	28	48	148	36	2.82	5.08	135	138	0.71	
KI (195°)	151	106	106	3.5	4.96	44	133	39	34	149	33	2.82	5.1	139	142		
KI (80°)	157	108	108	0.5	2.7	24	137	28	44	151	25	2.82	5.05	143	144.5		
KI (10°)	165	110	110	0.1	1.97			49	153	25	2.82	5.17	147	149			
RbI (300°)	103.5	75	75	2.2	2.8	31	92	21	35	105	16.5	2.71	4.84	99	100	0.73	
RbI (195°)	107	77	77	1.3	2.08	31	93	30	28	106	21	2.71	4.82	100	103		
RbI (80°)	108	80	80	0.1	1.45	31	94	30	18	108	17	2.71	4.67	103.5	105		
RbI (10°)	109	82	82	0.03	1.14	27	94	23	12	106	11	2.71	4.57	105.5	106.5		

^a From transmission measurements by Robert Lowndes (Ref. 21)!

¹⁷ R. C. Keezer, G. Lucovsky, and M. L. Slade, Solid State Commun. 6, 765 (1968).

¹⁸ R. G. J. Grisar, K. P. Reiners, W. F. Renk, and L. Genzel, Phys. Status Solidi 23, 613 (1967).

¹⁹ C. H. Perry, R. Geick, and E. F. Young, J. Appl. Optics 5, 1171 (1966).

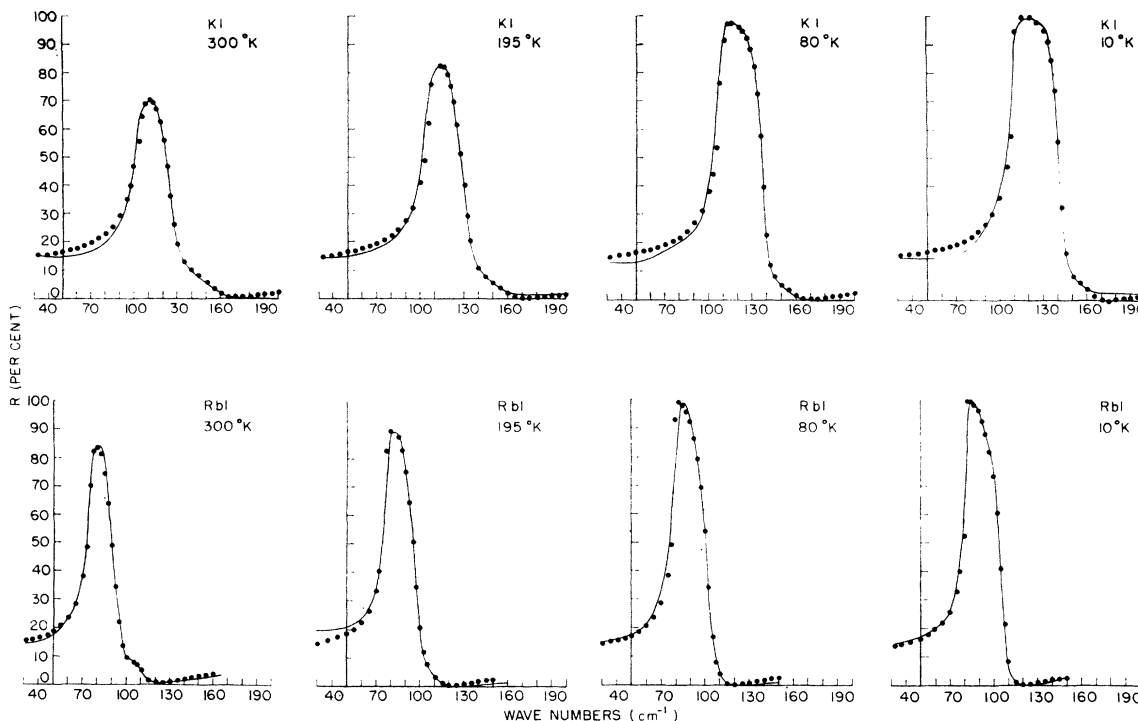


FIG. 2. Reflectivity spectra of KI and RbI at several temperatures; solid line denotes those observed, dotted line those calculated from the classical oscillator model.

measurements were made at an angle of incidence of 7.5° . The reflectivity curves shown in the figures are relative to the reflectivity of a front-aluminized reference mirror. The temperature was measured with a calibrated copper-constantan thermocouple. A germanium resistance thermometer was attached to the back of the samples.

III. EXPERIMENTAL RESULTS

A. Optical Constants of Pure End-Member Materials

The measured reflectivity spectra of KCl, KBr, KI, and RbI single crystals are shown in Fig. 1 and 2 for $T = 10^\circ, 80^\circ, 195^\circ,$ and 300°K . The main reststrahl peak can be identified as the transverse optical fundamental of frequency ω_T at the zone center. Also, all of the alkali halides show a sideband on the high-frequency side of the main peak.

The reststrahl bands have been fitted by computer programming to the classical dispersion formula

$$\epsilon(\omega) = \epsilon_\infty + \sum_i \frac{S_i^2}{\omega_i^2 - \omega^2 + i\omega\gamma_i} = \epsilon' + i\epsilon'' \quad (1)$$

where S_i is the oscillator strength $S_i^2 = \epsilon_i''\omega_i\gamma_i$, ω_i the transverse frequency, and γ_i the damping constant (resonance half-width) of oscillator i . It was found that a reasonable fit could not be obtained without assuming the existence of a second sideband between the main peak and the observed sideband. The dispersion con-

stants obtained in this way are shown in Table I. The frequencies ω_1 and ω_2 are undoubtedly due to multiphonon combinations at the zone edge, although no correlation could be obtained with the second-order Raman spectrum.²⁰

Here, the subscript T refers to the main transverse-lattice frequency, ϵ_∞ is the high-frequency dielectric constant, and ϵ_0 is the static dielectric constant; all frequencies are in cm^{-1} . For comparison, we have included the transverse-optical-phonon frequency ω_{TR} , and the associated damping constant γ_{TR} obtained by Lowndes²¹ from transmission measurements. ω_L is the frequency of the longitudinal optical fundamental at the zone center, and $\omega_L(\text{LST})$ is that same quantity calculated from the Lyddane-Sachs-Teller relation,²²

$$\omega_L(\text{LST}) = (\epsilon_0/\epsilon_\infty)^{1/2}\omega_T \quad (2)$$

The effective charge on an ion e^* is obtained from the Szigetti relation²³

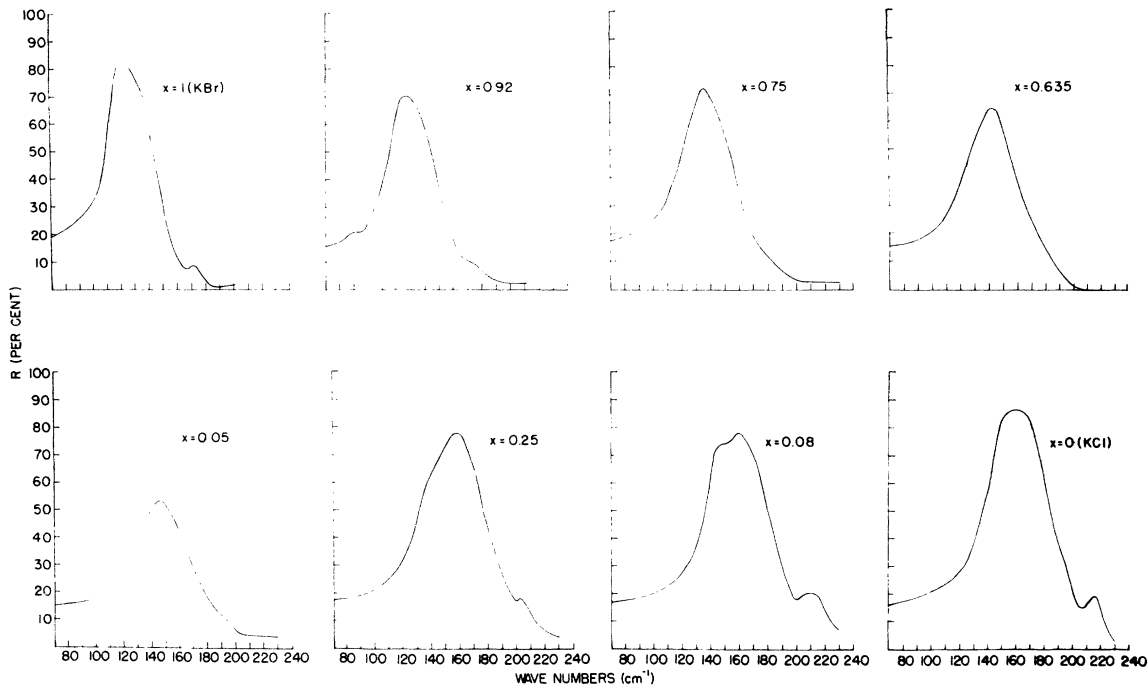
$$\omega_T^2 = \frac{4\pi N}{9\mu} \frac{e^{*2}(\epsilon_\infty + 2)^2}{\epsilon_0 - \epsilon_\infty} \quad (3)$$

²⁰ E. Burstein, F. A. Johnson, and R. Loudon, *Phys. Rev.* **139**, A1239 (1965).

²¹ R. P. Lowndes, Ph.D. thesis, University of London, 1967 (unpublished); R. P. Lowndes and D. H. Martin, *Proc. Roy. Soc. (London)* **A308**, 473 (1969).

²² R. H. Lyddane, R. G. Sachs, and E. Teller, *Phys. Rev.* **59**, 673 (1941).

²³ B. Szigetti, *Trans. Faraday Soc.* **45**, 155 (1949).

FIG. 3. Reflectivity spectra of $\text{KCl}_{1-x}\text{Br}_x$ at 300°K.

where N is the number of ion pairs per unit volume, and μ is the reduced mass of an ion pair.

B. $\text{KCl}_{1-x}\text{Br}_x$

The reststrahl bands of KCl and KBr overlap, and $m_{\text{Cl}} > \mu_{\text{KBr}}$. In addition, KCl does not have a gap in its

TABLE II. Dispersion constants for $\text{KCl}_{1-x}\text{Br}_x$ from Kramers-Kronig analysis.

X (mole fraction)	T (°K)	ϵ_0	ϵ_∞	ω_{TO}	ω_{LO}	γ
1	300	6.5	1.86	113.5	157.5	6
	195	6.3	1.86	117.5	161	3
	80	6.1	1.85	120	165	3
0.92	300	5.4	2.45	121	161	6
	195	5.6	2.43	124	167.5	4
	80	6.3	2.36	126	172	2.5
0.75	300	5.8	2.43	128	183	9
	195	6.12	2.4	129	184.5	8.5
	80	6.12	2.4	131	181.5	6.5
0.5	300	5.1	2.27	140	196	16
	195	5.1	2.23	143	197	12
	80	7.4	2.13	138	198	11.5
0.25	300	5.9	2.17	142	197.5	10
	195	6.12	2.15	143	203	9.5
	80	6.5	2.11	145	210	7
0.08	300	5.8	2.02	144	197	7
	195	5.8	2.0	147	205	4.5
	80	6.7	1.94	148	211	3
0	300	5.4	1.24	141	201	11
	195	5.78	2.68	154	208	14.5
	80	4.24	1.78	155	217.5	2.5

phonon spectrum, so no gap modes can arise at $x=0$. Thus, all three of the criteria mentioned above predict one-mode behavior for $\text{KCl}_{1-x}\text{Br}_x$. This result is observed.

Reflection measurements were made on crystals grown from the melt. The resulting spectra are shown in Fig. 3 for $T=300^\circ\text{K}$. At lower temperatures the damping constant decreases slightly, but the same general shape is observed. Only one main mode appears. The dispersion constants were obtained from a Kramers-Kronig analysis of the reflectance spectra and are listed in Table II.

Attempts were made to observe these materials in transmission by evaporating the powdered mixed crystal onto quartz and polyethylene substrates. Unfortunately, although one-mode behavior was observed, the frequencies of the transmission minima were all considerably higher than those obtained from the K-K analysis of the reflection measurements. It appeared that the composition of the thin films was not the same as that of the starting material, but had a higher percentage of KCl.

C. $\text{K}_{1-x}\text{Rb}_x\text{I}$

As previously mentioned, this is the only alkali halide mixed crystal whose end-member reststrahl bands do not overlap. It also satisfies Chang and Mitra's inequality and LBB's local-gap mode conditions—at least in one dimension.

Small mixed crystals of $\text{K}_{1-x}\text{Rb}_x\text{I}$ were obtained by dissolving appropriate amounts of the end-member

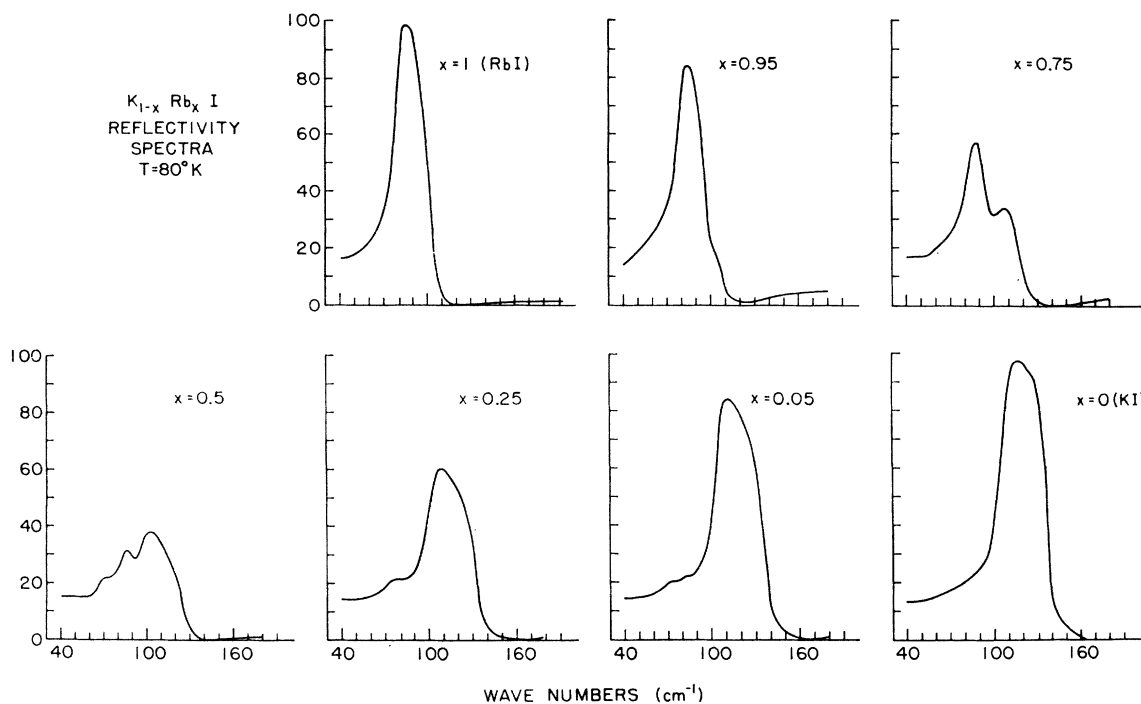


Fig. 4. Reflectance spectra of $K_{1-x}Rb_xI$ at $80^\circ K$.

compounds in distilled water and evaporating to dryness. The powders were then dried and pressed into pellets approximately 12 mm in diam and 1–2 mm thick. The samples were examined using x-ray techniques, and

the results indicate that KI and RbI do form solid solutions over the entire composition range, and that the lattice constant changes linearly with composition. Reflection measurements were made at 300, 195, and

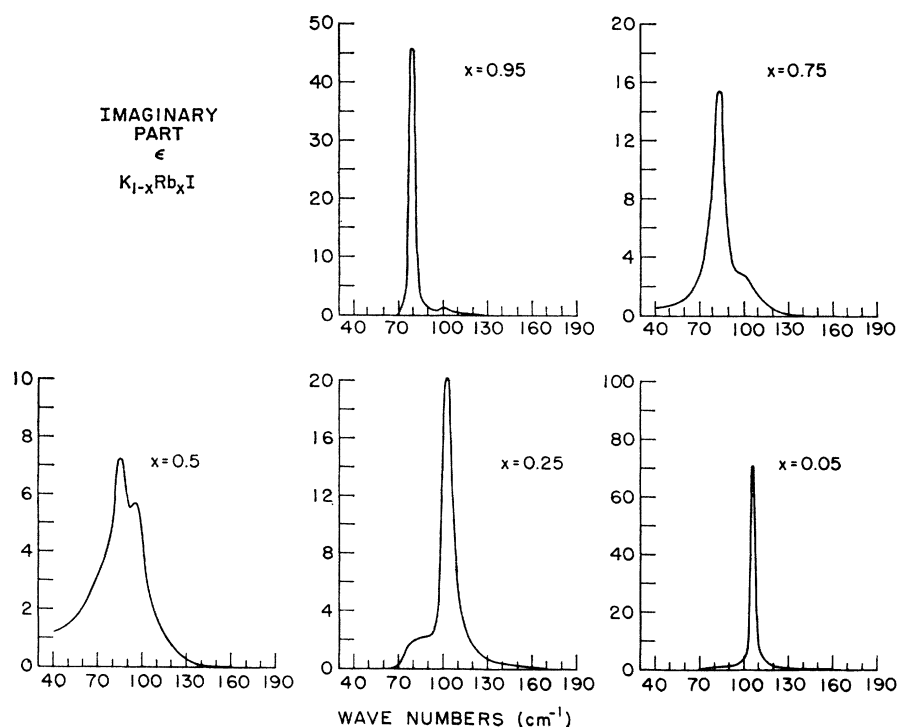


Fig. 5. Imaginary part of the dielectric constant for $K_{1-x}Rb_xI$ obtained from Kramers-Kronig analysis.

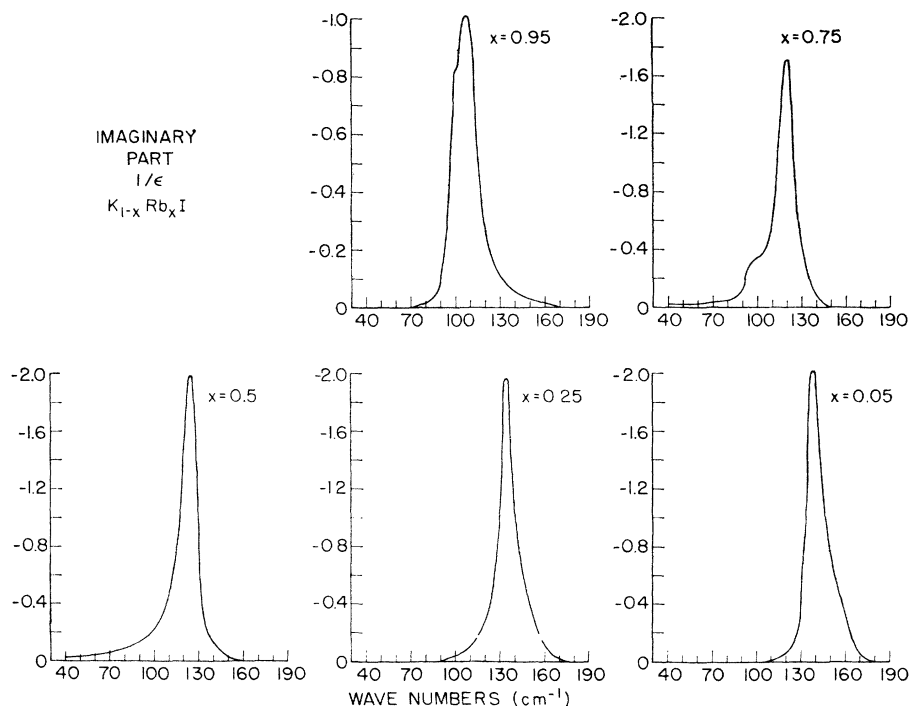


FIG. 6. Imaginary part of the reciprocal of the dielectric constant of $K_{1-x}Rb_xI$ obtained from Kramers-Kronig analysis.

80°K. The resulting spectra at 80°K are shown in Fig. 4. The results of a Kramers-Kronig analysis of the reflectivity data are shown in Fig. 5. The maxima of the imaginary part of the dielectric constant ϵ'' determine the TO frequencies. (Actually, the TO frequency lies between the maximum of ϵ'' and that of $\omega\epsilon''$, but these values are only about 0.5 cm^{-1} apart.) Two-mode behavior is observed over almost the entire composition range.

The position of the LO modes is determined from peaks in η'' , the imaginary part of the reciprocal of the dielectric constant plotted in Fig. 6. (The LO frequency actually lies between the maximum of η'' and that of $\omega\eta''$, but again these values are only about 0.5 cm^{-1} apart.) Only one LO mode appears for most of the samples, although the crystals with $x=0.75$ and 0.95 show some indication of a second mode. The TO and LO frequencies obtained in this way are listed in Table III.

Normal incidence thin-film transmission measurements of these materials also showed two-mode behavior for the TO modes, and the composition of the thin films seemed to be consistent with the starting material. The measurement of the LO frequency was obtained by using Berreman's technique²⁴ of oblique-incidence reflection (average angle of incidence $\sim 75^\circ$) of a thin film evaporated onto a mirror, using the radiation polarized in the plane of incidence. The results of the thin film measurements are shown in Fig. 7. The small sidebands on the low-frequency side of the LO mode are probably due to the angle of inci-

dence causing some small interaction of the radiation with the TO modes. The band labeled P is due to polyethylene (the vacuum windows in the oblique-incidence cryostat), which was not completely removed in the ratioing process.

TABLE III. Frequencies for $K_{1-x}Rb_xI$ from Kramers-Kronig analysis.

X (mole fraction)	T (°K)	$\omega_{TO}^{(1)}$	$\omega_{TO}^{(2)}$	$\omega_{LO}^{(2)}$	$\omega_{LO}^{(1)-calc.}$
1	300	75		99	
	195	77		100	
	80	80		103.5	
0.95	300	74		99	90
	190	76		103	
	80	79	101	107	
0.75	300	78	94	115	85.5
	195	81	97	117	
	80	83	98	120	
0.5	300	84	94	123	86
	195	88	98	127	
	80	85	96	125	
0.25	300	84	100	131	86
	195	83	102	133	
	80	84	103	135	
0.05	300		102	132	89
	195		105	136	
	80		106	139	
0	300	88 ^a	103.5	135	
	195		106	139	
	80		108	143	

²⁴ D. W. Berreman, Phys. Rev. **130**, 2193 (1963).

^a Reference 25.

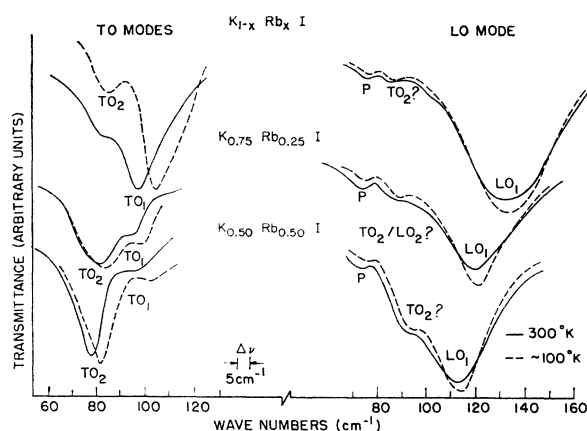


FIG. 7. Transmission spectra for some of the $K_{1-x}Rb_xI$ samples. The LO modes were obtained using Berreman's technique.

Figure 8 shows the variation of frequency with composition for measurements taken at room temperature. It can be seen that the agreement between the Kramers-Kronig data from the reflection measurements and the transmission data from the thin films is quite good. The gap mode labeled G of Rb^+ in KI was calculated from data provided by Genzel,²⁵ and agrees well with the value obtained by extrapolating the TO_2 mode

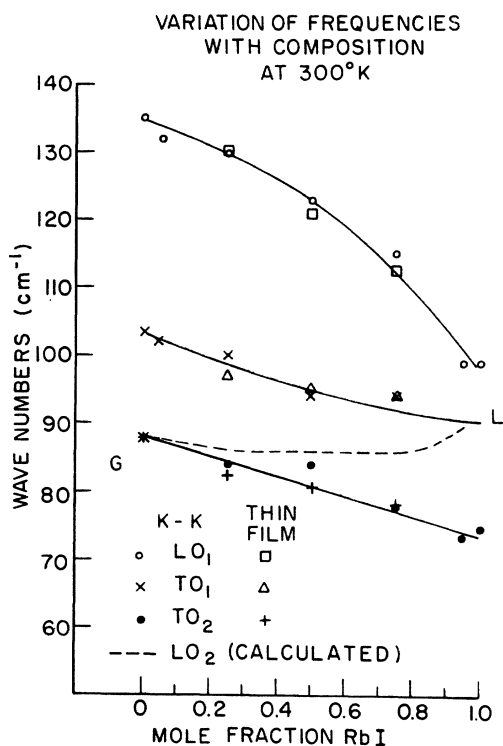


FIG. 8. Variation of room-temperature frequencies of $K_{1-x}Rb_xI$ with composition.

²⁵ L. Genzel (private communication).

to $x=0$. The dotted line shows where the LO_2 mode should appear according to the modified Lyddane-Sachs-Teller relation²⁶;

$$\frac{\epsilon_{\infty}}{\epsilon_0} = \prod_f \frac{\omega_{Tf}^2}{\omega_{Lf}^2} \quad (4)$$

This mode is probably unobservable since it is much weaker than the LO_1 and close to both TO modes. The point labeled L shows roughly where a localized mode of K^+ in RbI would appear. This, however, is between the RbI LO and TO frequencies, so that, no such mode arises. Thus, $K_{1-x}Rb_xI$ does not, in fact, satisfy the local-gap mode condition of LBB in three dimensions.

IV. APPLICABILITY OF VARIOUS THEORETICAL MODELS

Several models have been proposed to describe the frequency variation in mixed-crystal systems. A linear chain model was used by Matossi,²⁷ who calculated the vibrational frequencies of a one-dimensional ordered diatomic 50-50 mixed crystal $-A-C-A-B-A-C-A-B-$. Only nearest-neighbor interactions were considered and the force constants were obtained from the frequencies of the pure end-member compounds. Thus, shifts in the calculated frequency spectra derive solely from the mass differences in the isotopic substitution which generates the mixed crystal. When the mass of A is much heavier than the masses of B and C (such as for $K_{1-x}Rb_xI$), two infrared frequencies are obtained which are very close to those of the end-member compounds. On the other hand, for $KCl_{1-x}Br_x$ the model predicts one infrared active mode at a frequency approximately halfway between the frequencies of the end members, and another (weaker) one at a much lower frequency. The higher-frequency mode predicted by this model for 50-50 crystals in the case of

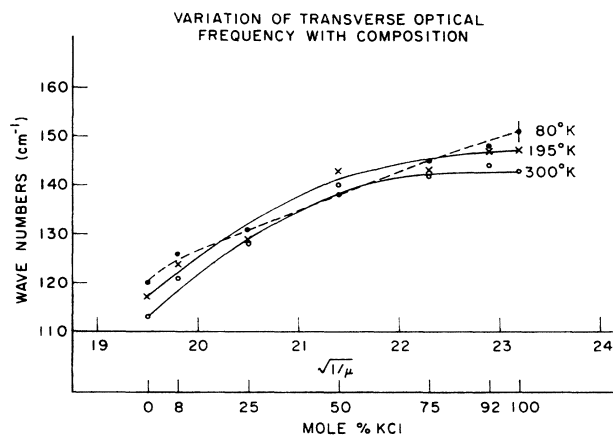


FIG. 9. Variation of $KCl_{1-x}Br_x$ transverse optical frequency with reduced mass. $\circ = 300^\circ K$, $\times = 195^\circ K$, $\bullet = 80^\circ K$.

²⁶ A. S. Barker, Jr., Phys. Rev. **136**, A1290 (1964).

²⁷ F. Matossi, J. Chem. Phys. **19**, 161 (1951).

both $\text{KCl}_{1-x}\text{Br}_x$ (134 cm^{-1}) and $\text{K}_{1-x}\text{Rb}_x\text{I}$ (99 cm^{-1}) agrees quite well with the experimental data. However, in the case of $\text{K}_{1-x}\text{Rb}_x\text{I}$ the predicted value for the lower-frequency mode (64.8 cm^{-1}) is well removed from the observed frequency. For $\text{KCl}_{1-x}\text{Br}_x$, the weak lower-frequency mode (79 cm^{-1}) could not be observed at all, even in transmission of samples 1 mm thick at 10°K . The Raman active mode predicted by the linear chain model was also not observed, but this may be due to the fact that the crystals are not perfectly ordered.

The virtual crystal model²⁸ can only be used to describe one-mode behavior. All masses and spring constants are taken as averages weighted by the mixed crystal composition. One mode is predicted whose frequency varies linearly with the reciprocal of the square root of the reduced mass. Although Figs. 9 and 10 show that the $\text{KCl}_{1-x}\text{Br}_x$ frequencies do not show such a linear variation, the virtual crystal model does successfully predict the variation of the damping with composition, and is, in fact, the only model capable of determining phonon lifetimes. The resonance half-width is predicted to vary linearly with q , where q is the fraction of the less common mass. Figure 11 shows that this is indeed what happens, except for the sample with $x=0.635$, whose damping constant is anomalously high. An x-ray examination of this crystal showed that it was not homogeneous, but consisted of two phases of slightly different composition.

The random element isodisplacement (REI) model⁸ assumes that each of the atomic species vibrates with the same phase and amplitude. Four constants are needed to fit the model to any given mixed crystal. For the crystal $\text{AB}_{1-x}\text{C}_x$, the force constant F_{p0} between the A and B sublattices and that between the A and C sublattices (F_{a0}) are determined by the frequencies of the end-member compounds. The third constant θ describes how the force constants vary with the lattice

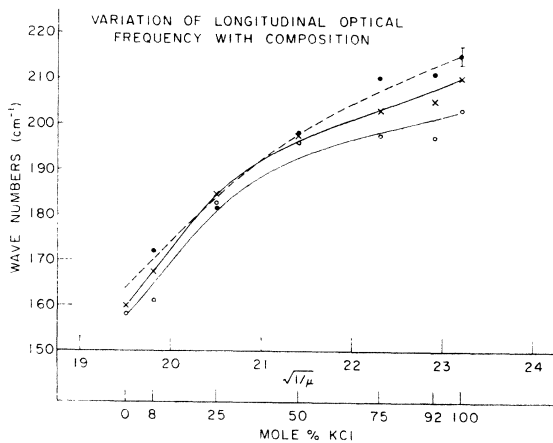


FIG. 10. Variation of $\text{KCl}_{1-x}\text{Br}_x$ longitudinal optical frequency with reduced mass. $\circ = 300^\circ\text{K}$, $\times = 195^\circ\text{K}$, $\bullet = 80^\circ\text{K}$.

²⁸ J. S. Langer, J. Math. Phys. 2, 584 (1961).

VARIATION OF DAMPING CONSTANT WITH COMPOSITION AND TEMPERATURE

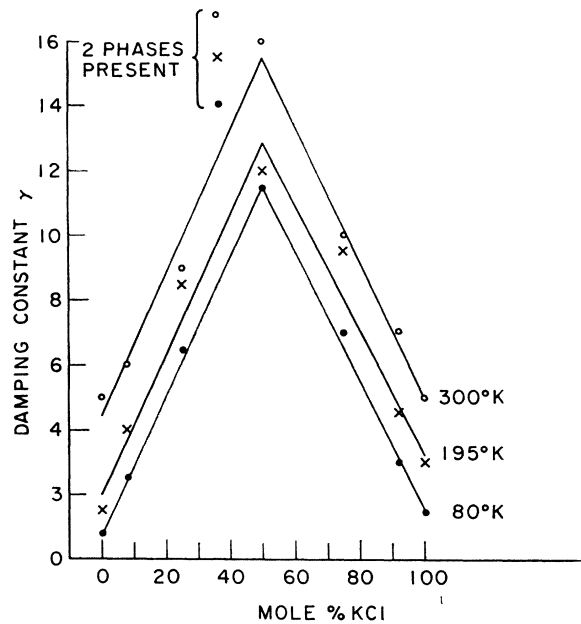


FIG. 11. Variation of resonance half-width of $\text{KCl}_{1-x}\text{Br}_x$ with composition; Solid line was calculated from virtual-ion model, \times 's are experimental points—from Kramers-Kronig analysis of reflection data. The sample with $x=0.635$ turned out to be nonhomogeneous.

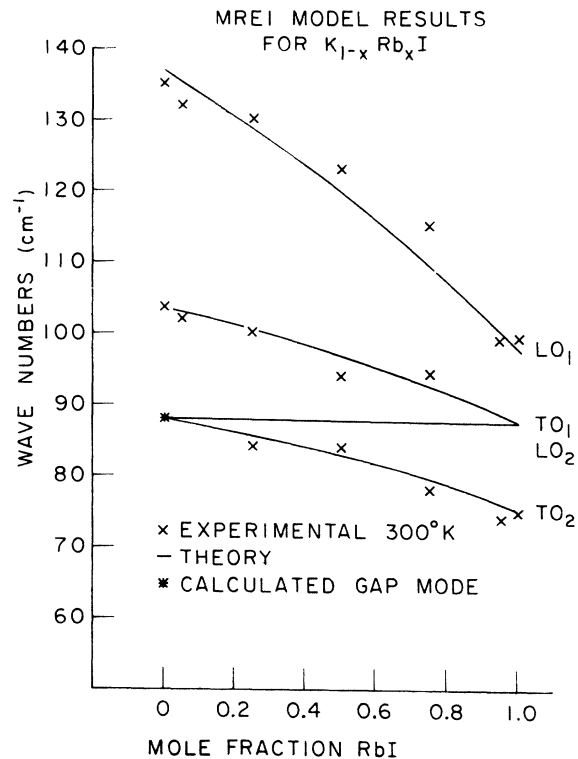


FIG. 12. MREI-model results for TO and LO modes of $\text{K}_{1-x}\text{Rb}_x\text{I}$.

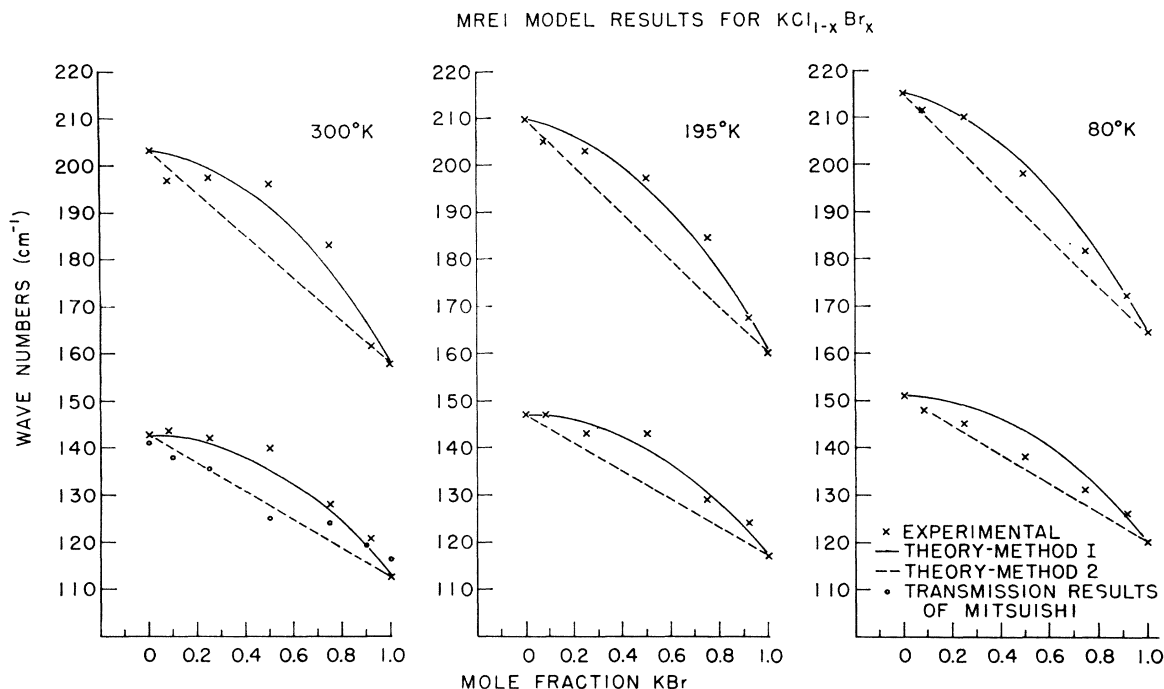


Fig. 13. MREI-model results for TO and LO modes of $\text{KCl}_{1-x}\text{Br}_x$ at three temperatures. The upper curves are obtained using method 1, the lower curves (almost straight lines) are from method 2.

dimensions, and is calculated from the Gruneisan constant. The force constant F_{s0} between the B and C sublattices is then treated as an adjustable parameter which can be varied to give the best fit to the observed data. Since all these force constants are really effective force constants, the effects of next-nearest-neighbor and higher-order interactions are included. In the case of $\text{K}_{1-x}\text{Rb}_x\text{I}$, the model can be made to fit the data quite satisfactorily, and predicts the correct frequency dependence, with composition for the two observed modes. The best value obtained for F_{s0} is of the same order of magnitude as those calculated for the K-I and Rb-I interactions. However, the fit of the model to the $\text{KCl}_{1-x}\text{Br}_x$ data is less successful. In particular, a second mode occurring at lower frequency is predicted in addition to the main mode, and even the calculated frequency variation for the mode that is observed is not in good agreement with the data.

The modified REI (MREI) model¹⁵ differs from the REI model in that it contains no variable parameters and does not make use of the Gruneisan constant. Instead, the third and fourth constants described above are calculated from the frequencies of the gap and local modes at $x=0$ and $x=1$. It is also possible to obtain the LO frequencies by including the polarization field. Since, as already mentioned, there is no local mode of K^+ in RbI , this frequency had to be used as a variable to be determined by a best fit to the data. In this case, therefore, the MREI model is the same as the REI model, except that the gap-mode frequency of Rb^+ in KI is

used in place of the Gruneisan constant. The best fit obtained for $\text{K}_{1-x}\text{Rb}_x\text{I}$ is quite satisfactory, and is shown in Fig. 12. The frequency predicted for the local mode of K^+ in RbI is 87.5 cm^{-1} . This is consistent with the fact that such a mode is not observed as it is within the RbI optical band.

Since there are no local and gap modes in one-mode systems, additional conditions have to be imposed in order to determine the four constants. Either the two roots of the secular equation determining the frequencies can be set equal to each other (method 1), or one root can be set equal to zero (method 2). In the latter instance, the MREI model reduces to the virtual crystal model. Although Chang and Mitra claim that all the known one-mode systems conform to the predictions of method 2, our results for $\text{KCl}_{1-x}\text{Br}_x$, shown in Fig. 13, seem to be best described by method 1, except at 80°K where neither method is adequate. For comparison, we include Mitsubishi's thin-film transmission measurements²⁹ which do seem to follow the virtual crystal predictions. These results may not be very reliable, however, because of the already mentioned difficulty of accurately knowing the composition of the film.

V. EVALUATION OF CRITERIA FOR ONE- AND TWO-MODE BEHAVIOR

$\text{K}_{1-x}\text{Rb}_x\text{I}$ does not satisfy the local-gap mode criterion of LBB, yet it shows two-mode behavior.

²⁹ A. Mitsubishi, in U. S.-Japan Cooperative Seminar on Far Infrared Spectroscopy, Columbus, Ohio, 1965 (unpublished).

Thus, it is apparent that this condition, while it may be sufficient, is not really necessary for the appearance of two modes.

Chang and Mitra's inequality, on the other hand, is satisfied by $K_{1-x}Rb_xI$, but this condition also predicts two-mode behavior for $K_{1-x}Rb_xBr$ and $RbCl_{1-x}Br_x$. The reflectivity spectra of the $x=0.5$ crystal of both these systems are shown in Figs. 14 and 15, and it is obvious that these are both one-mode systems. Therefore, this criterion ($m_B < \mu_{AC}$) is not by itself a sufficient condition for two-mode behavior.

It should be noted, however, that the reststrahl bands of the end members of $K_{1-x}Rb_xI$ do not overlap while those of $K_{1-x}Rb_xBr$ and $RbCl_{1-x}Br_x$ do. As already mentioned, two-mode behavior has *never* been observed for systems which have frequency overlap, and it is desirable to include this fact in formulating conditions for two-mode behavior. The results for all mixed systems so far observed will be correctly predicted, if it is assumed that two-mode behavior will appear if and only if $m_B < \mu_{AC}$, and there is no frequency overlap between the reststrahl bands of the end members.

Note added in proof. This criterion can be given a more rigorous basis in the following manner. It has already been pointed out that even if the inequality $m_B < \mu_{AC}$ is satisfied a local mode may not appear at $x=1$, since although the local mode frequency of B in AC is higher than the TO frequency of AC , it will not necessarily be higher than the LO frequency of AC . In order to ensure that $\omega_{local} > \omega_{LO}(AC)$, the inequality

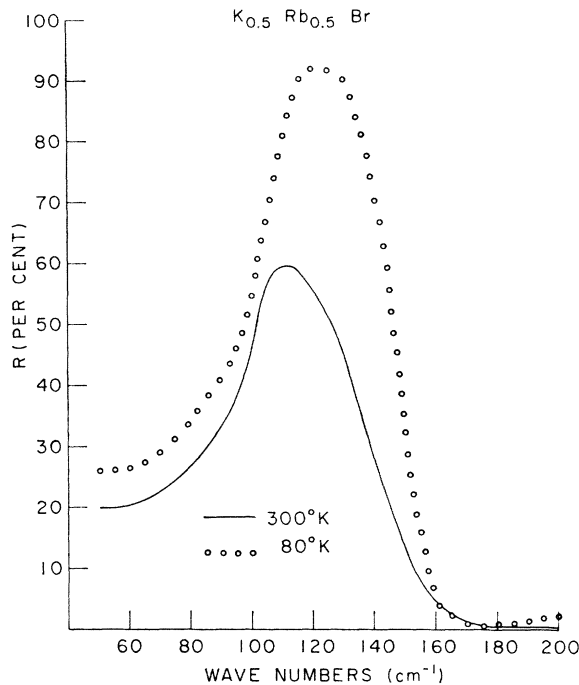


FIG. 14. Reflectivity spectra of $K_{0.5}Rb_{0.5}Br$ at two temperatures.

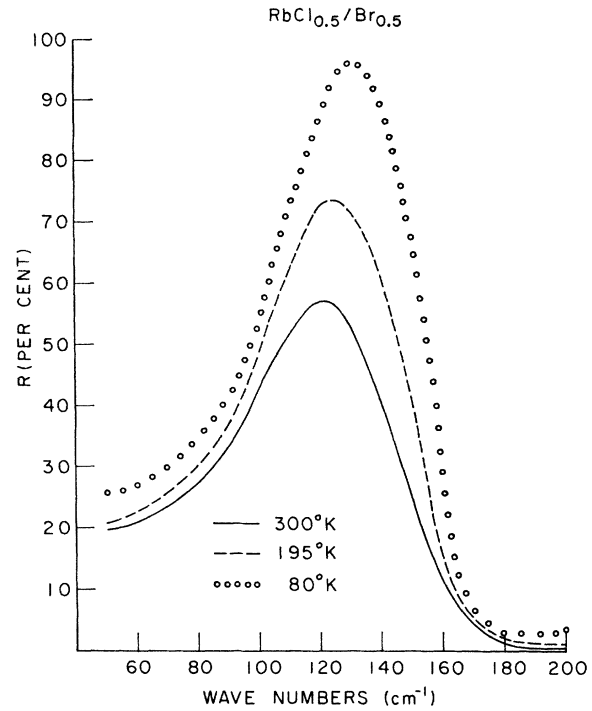


FIG. 15. Reflectivity spectra of $RbCl_{0.5}Br_{0.5}$ at three temperatures.

that must be satisfied is

$$\begin{aligned} \omega_{local} &= \frac{F_{ABO} + F_{BCO}}{m_B} (1 - \theta) > \omega_{LO}(AC) \\ &= \left(\frac{\epsilon_0(AC)}{\epsilon_\infty(AC)} \right)^{1/2} \omega_{TO}(AC) \\ &= \left(\frac{\epsilon_0(AC)}{\epsilon_\infty(AC)} \right)^{1/2} \frac{F_{ACO}}{\mu_{AC}} (1 - \theta), \quad (5) \end{aligned}$$

assuming that the Lyddane-Sachs-Teller relation gives an accurate value for the LO frequency. If all the force constants are of the same order of magnitude (which is usually the case), we are led to the following condition for two-mode behavior:

$$m_B < [\epsilon_\infty(AC) / \epsilon_0(AC)]^{1/2}, \quad (6)$$

which is stronger than that of Chang and Mitra.¹⁵

It can also be shown that if the inequality (6) is satisfied, the reststrahl bands of the end members will not overlap. The condition for nonoverlap is $\omega_{TO}^2(AB) > \omega_{LO}^2(AC)$, and according to the MREI model formulation, this can be rewritten as

$$\frac{F_{ABO}}{\mu_{AB}} > \frac{F_{ACO}}{\mu_{AC}} (1 - \theta) \left(\frac{\epsilon_0(AC)}{\epsilon_\infty(AC)} \right)^{1/2}. \quad (7)$$

In the same manner as before, we are led to

$$\mu_{AC} > \mu_{AB}(1-\theta)[\epsilon_0(AC)/\epsilon_\infty(AC)]^{1/2}, \quad (8)$$

which implies that

$$m_C > m_B(1-\theta)[\epsilon_0(AC)/\epsilon_\infty(AC)]^{1/2}, \quad (9)$$

or

$$m_C[\epsilon_\infty(AC)/\epsilon_0(AC)]^{1/2} > m_B(1-\theta). \quad (10)$$

Since $m_C[\epsilon_\infty(AC)/\epsilon_0(AC)]^{1/2} > \mu_{AC}[\epsilon_\infty(AC)/\epsilon_0(AC)]^{1/2}$ and $m_B(1-\theta) < m_B$, we have

$$m_C[\epsilon_\infty(AC)/\epsilon_0(AC)]^{1/2} > \mu_{AC}[\epsilon_\infty(AC)/\epsilon_0(AC)]^{1/2} > m_B > m_B(1-\theta). \quad (11)$$

Thus it is apparent that the nonoverlap requirement is a less restrictive condition than the requirement of inequality (6) and is included in it.

ACKNOWLEDGMENTS

We wish to thank Professor A. Smakula of the MIT Center for Materials Science and Engineering for the pure alkali halides and $\text{KCl}_{1-x}\text{Br}_x$ samples, and J. Kalnajs for the x-ray measurements and their interpretation. This work forms a part of the thesis of one of us (J.H.F.) to be submitted to the MIT Physics Department in partial fulfillment of the requirements for the Ph.D. degree.

Theory of the Self-Trapped Hole in the Alkali Halides*

A. NORMAN JETTE

Applied Physics Laboratory, The Johns Hopkins University, Silver Spring, Maryland 20910

AND

T. L. GILBERT

Argonne National Laboratory, Argonne, Illinois 60439

AND

T. P. DAS

Department of Physics, University of California, Riverside, California 92502

(Received 7 February 1969)

Combining the self-consistent-field molecular-orbital results for the wave functions and energies of F_2^- and Cl_2^- with a classical calculation of the lattice distortion and polarization energies, we have obtained the ground- and excited-state potential curves of the V_K center in several of the alkali halides. The widths and peak values of the optical-absorption bands have been calculated from these potential curves and are found to be in reasonable agreement with, but somewhat smaller than, the experimental results. The hyperfine constants are obtained as a function of internuclear distance and compared with the experimental results using the internuclear distance at the minimum of the configurational coordinate curves. The significance of the remaining discrepancies between theory and experiment for interpreting still unresolved aspects of the structure of V_K centers is pointed out.

I. INTRODUCTION

THE study of the structure and properties of color centers continues to be a fruitful area of theoretical and experimental research in solid state physics. This study has been made possible by new experimental techniques which provide more accurate probes into properties that were studied earlier and that have also made possible the measurement of properties that were not accessible previously. The experimental results have raised new problems which have stimulated theorists to try to gain further understanding of the structure of these interesting systems and of defects in ionic crystals in general. Efforts in this direction have

been helped by refinements in our theoretical understanding of atomic and molecular systems and the rapid advancements in computer technology, which have added a dimension to efforts in the theory of the solid state. The two centers that have been studied most extensively are the F center and its close associates,¹⁻⁴ and the self-trapped hole or V_K center.^{1,2} The present work is concerned with the theory of this latter type of center.

¹ W. Beall Fowler, in *Physics of Color Centers*, edited by W. Beall Fowler (Academic Press Inc., New York, 1968).

² J. H. Schulman and W. D. Compton, *Color Centers in Solids* (Pergamon Publishing Corp., New York, 1962).

³ B. S. Gourary and F. J. Adrian, in *Solid State Physics*, edited by F. Seitz and D. Turnbull (Academic Press Inc., New York, 1960), Vol. 10.

⁴ J. J. Markham, *F-Centers in Alkali Halides* (Academic Press Inc., New York, 1966).

* Work supported in part by the National Science Foundation, the U. S. Atomic Energy Commission, and the Bureau of Naval Weapons, U. S. Department of the Navy, under Contract No. NOW 62-0604-c.